MS4A12 Is a Colon-Selective Store-Operated Calcium Channel Promoting Malignant Cell Processes

Michael Koslowski,[1] Ugur Sahin,[1] Karl Dhaene,[3] Christoph Huber,[1] and Özlem Türeci[2]

[1]Department of Internal Medicine III, Division of Experimental and Translational Oncology, Johannes Gutenberg University; [2]Ganymed Pharmaceuticals AG, Mainz, Germany; and [3]Institute of Pathology, Algemeen Stedelijk Ziekenhuis, Aalst, Belgium

Abstract

Using a data mining approach for the discovery of new targets for antibody therapy of colon cancer, we identified MS4A12, a sequence homologue of CD20. We show that MS4A12 is a cell surface protein. Expression analysis and immunohistochemistry revealed *MS4A12* to be a colonic epithelial cell lineage gene confined to the apical membrane of colonocytes with strict transcriptional repression in all other normal tissue types. Expression is maintained upon malignant transformation in 63% of colon cancers. Ca^{2+} flux analyses disclosed that MS4A12 is a novel component of store-operated Ca^{2+} entry in intestinal cells. Using RNAi-mediated gene silencing, we show that loss of MS4A12 in LoVo colon cancer cells attenuates epidermal growth factor receptor–mediated effects. In particular, proliferation, cell motility, and chemotactic invasion of cells are significantly impaired. Cancer cells expressing MS4A12, in contrast, are sensitized and respond to lower concentrations of epidermal growth factor. In summary, these findings have implications for both the physiology of colonic epithelium as well as for the biology and treatment of colon cancer. [Cancer Res 2008;68(9):3458–66]

Introduction

Antibody-based cancer therapies have been successfully introduced into the clinic and have emerged over the last decade as the most promising therapeutics in oncology (1). Hematologic malignancies provided a successful testing ground for therapeutic concepts based on monoclonal antibodies (mAb). In these diseases antigens, which are expressed exclusively on a particular lineage of hematopoetic cells, such as CD20, CD22, CD25, CD33, and CD52 (2–4), have proven as useful therapeutic targets. Most prominent among these are anti-CD20 mAbs as they have revolutionized the treatment of lymphoma patients. The chimeric anti-CD20 mAb rituximab has achieved response rates of ~40% to 60% in patients with multiply relapsed indolent B-cell lymphomas and has become the first mAb approved by the U.S. Food and Drug Administration for the treatment of cancer (4). The spectrum of lymphoproliferative disorders eligible for CD20-targeting therapy is still growing (5).

Two key characteristics contribute to the clinical success of CD20 as an antibody target. First, this target provides an optimal therapeutic window, as it is a highly selective differentiation marker for the B-cell lineage. CD20 expression is neither detectable on any other normal cell type nor on the stem cell precursor of the B-cell lineage (6). Accordingly, there is no severe dose-limiting toxicity and normal B-lymphocyte levels are eventually restored by target-negative stem cells. B-cell malignancies, which in general preserve expression of this differentiation antigen, can be treated successfully. The second peculiarity is that compared with other mAbs against hematopoetic differentiation antigens, anti-CD20 antibodies are of unusual high cytocidal potency (7). At least *in vitro*, they mediate both complement-dependent cytotoxicity and antibody-dependent cell-mediated cytotoxicity. Efficient recruitment of cellular and soluble immune effectors seems to be closely linked to the characteristic membrane topology of the CD20 molecule accounting for a high lateral mobility of antibody/antigen complexes and a short distance between the target epitope and the lipid bilayer (7–9). In addition to recruiting immune effectors, anti-CD20 mAbs are able to mediate growth arrest and apoptosis in certain cell lines (10–13). Mechanisms by which anti-CD20 mAbs interfere with proliferation and survival remained unknown until recently, when CD20 was established as a component of a store-operated Ca^{2+} (SOC) entry pathway activated by the B-cell receptor.

Intracellular Ca^{2+} is an essential regulator of cell function. Signaling through growth receptors leads to rapid release of Ca^{2+} from intracellular stores into the cytoplasm. Store depletion activates Ca^{2+} influx across the plasma membrane, replenishing empty stores and providing a sustained increase in the concentration of cytoplasmic free Ca^{2+} ($[Ca^{2+}]_c$). This Ca^{2+} influx has been termed capacitative or SOC entry and is essential for regulating diverse cellular responses to receptor-mediated stimuli, including survival and proliferation (14–16). In line with the role of CD20 in modulation of Ca^{2+} signaling, it has been shown that Ca^{2+} influx is essential for rituximab-induced antiproliferative and apoptotic effects (12, 17, 18).

Lessons learned from anti-CD20 antibodies and rationales developed in hematologic diseases may empower the design of rational mAb therapies in solid cancer with still high medical need. However, for solid tumors, targets of analogous potency are not yet available. A data mining strategy for discovery of differentiation genes of colonic epithelia exploitable as targets for therapeutic antibodies in colon cancer led us to *MS4A12*, a close relative of *CD20*. We show here that *MS4A12* is a colonocyte-specific differentiation gene involved in SOC entry, which functions as a novel modulator of epidermal growth factor receptor (EGFR) signaling. Our data give unexpected insights into the physiology of colonic epithelial cells and into the biology of colon cancer and may provide a novel target candidate for the treatment of colon cancer.

Materials and Methods

Tissues and cell lines. Recombinant DNA work was done with the official permission and according to the rules of the state government of

Note: Supplementary data for this article are available at Cancer Research Online (http://cancerres.aacrjournals.org/).

U. Sahin and Ö. Türeci contributed equally.

Requests for reprints: Özlem Türeci, Ganymed Pharmaceuticals AG, Freiligrathstr. 12, 55131 Mainz, Germany. Phone: 49-6131-1440100; Fax: 49-6131-1440111; E-mail: oe.tuereci@ganymed-pharmaceuticals.com.

doi:10.1158/0008-5472.CAN-07-5768

Rhineland-Palatinate. Fresh-frozen tissues were obtained as human surplus materials during routine diagnostic or therapeutic procedures. Precautions were taken to avoid prolonged exposure and tissues were stored at −80°C until use. Colon cancer cell line LoVo was cultured in DMEM + 10% fetal bovine serum.

Data mining strategy for discovery. As a first step, we created a general human expressed sequence tag (EST) file from all available libraries that contained the keyword "Homo sapiens" in the organism field of the dbEST report file.[4] To reduce complexity of the approach, only libraries representing >100 ESTs and only ESTs encoding known full-length genes were considered. Next, a colon tissue–specific subfile was generated by extracting all those ESTs from the general file that contained the words "colon" in the library name, organism, tissue type, organ, or cell line field. In total, we analyzed 6,280,883 ESTs represented in 4,021 cDNA libraries. To account for the fact that several EST may be derived from the same gene, the colon tissue ESTs were grouped into clusters, assembling ESTs that shared one or more stretches of high-sequence identity. The sequence homology searching program blastn[5] was run sequentially with the homology stringency set $S = 300$, $V = 300$, $B = 300$, $n = -20$ for each sequence recorded in the colon tissue EST subfile against all of the human ESTs in the general list. For each query EST from the colon tissue subfile, the search extracted a list of EST entries (hits) from the general EST file, each of them annotated with its tissue origin, providing an "electronic Northern." Determination of the number of different noncolon tissues represented in such a hit list was used as a measure for the extent of colon tissue specificity of each individual EST. All candidates obtained by this procedure were subjected to motif and structure analysis by SMART[6] to identify potential surface molecules. Candidates obtained by this procedure were subjected to motif and structure analysis by SMART to identify surface molecules topologically resembling CD20 (minimal requirements, at least four hydrophobic regions qualifying as transmembrane domains according to TMHMM, and prediction of at least one extracellular loop).

RNA isolation, reverse transcription-PCR, and real-time reverse transcription-PCR. RNA extraction, first-strand cDNA synthesis, reverse transcription-PCR (RT-PCR), and real-time RT-PCR were performed as previously described (19). For end point analysis, MS4A12-specific oligonucleotides (sense, 5′-GAG CTT TCC CGT TGT CTG GTG-3′; antisense, 5′-GCT GAA GAA GAC GCT GGT GTC-3′; 60°C annealing) were used in a 35 cycle RT-PCR. Real-time quantitative expression analysis was performed in triplicates in a 40 cycle RT-PCR. After normalization to hypoxanthine phosphoribosyltransferase (sense, 5′-TGA CAC TGG CAA AAC AAT GCA-3′; antisense, 5′-GGT CCT TTT CAC CAG CAA GCT-3′; 62°C annealing), MS4A12 transcripts in tumor samples were quantified relative to normal tissues using ΔΔCT calculation. Specificity of PCR reactions was confirmed by cloning and sequencing of amplification products from arbitrarily selected samples.

Antisera, immunofluorescence, and immunochemistry. The polyclonal antiserum was raised against recombinantly expressed fragment of MS4A12 (amino acids 1–63) and affinity purified by a custom antibody service (Squarix). Immunohistochemistry was performed on tissue cryosections using the VECTOR NovaRED Substrate kit (Vector) according to the manufacturer's instructions. For Western blot analysis, 20 μg of total protein extracted from cells lysed with Triton-X was used. Extracts were diluted in reducing sample buffer (Roth), subjected to SDS-PAGE, and subsequently electrotransferred onto polyvinylidene difluoride membrane (Pall). Immunostaining was performed with antibodies reactive to MS4A12, KRT18 (Abcam), and β-Actin (Abcam) followed by detection of primary antibody with horseradish peroxidase–conjugated goat anti-mouse and goat anti-rabbit secondary antibodies (Dako).

Small interfering RNA duplexes. Two individual MS4A12 small interfering RNA (siRNA) duplexes (Qiagen) targeting nucleotides 344 to 362 [siRNA#1; sense, 5′-r(UCA UGG UUG GAU UGA UGC A)dTdT-3′; antisense, 5′-r(UGC AUC AAU CCA ACC AUG A)dGdA-3′] and nucleotides 247 to 265 of the MS4A12 mRNA sequence [siRNA#2; sense, 5′-r(CAA CCG GGU CAA GGA AAU A)dTdA-3′; antisense, 5′-r(UAU UUC CUU GAC CCG GUU G)dAdC-3′] were designed. As control a nonsilencing siRNA duplex [sense, 5′-r(UAA CUG UAU AAU CGA CUA G)dTdT-5′; antisense, 5′-r(CUA GUC GAU UAU ACA GUU A)dGdA-3′] was used. For MS4A12 silencing studies, cells were transfected with 10 nmol/L siRNA duplex using HiPerFect transfection reagent (Qiagen) according to the manufacturer's instructions.

Calcium imaging. All buffers contained 125 mmol/L NaCl, 5 mmol/L KCl, 1 mmol/L $MgCl_2$, 20 mmol/L HEPES, and the pH was adjusted to 7.4 with NaOH. $CaCl_2$ and $SrCl_2$ were added to the buffer at 1 mmol/L final concentration as indicated. Ca^{2+}-free buffer contained 0.2 mmol/L EGTA. Thapsigargin, epidermal growth factor (EGF), and La^{3+} were used at the indicated concentrations. Fluorophore labeling of cells was conducted using FLIPR Calcium 3 Assay kit (Molecular Devices) according to the manufacturer's instructions. Changes in intracellular calcium were documented using Olympus-IX71 inverted microscope and TILLvisION software (TILL Photonics). Fluorescence values in a field of >50 cells were recorded during the perfusion of various reagents. All assays were done in quadruplicates and repeated twice.

Cell proliferation analysis. Twenty-four hours after transfection with siRNA duplexes, 1×10^4 cells were cultured in serum-free medium for 12 h. Forty-eight hours after medium was supplemented with EGF (50 nmol/L), proliferation was analyzed by measuring the incorporation of BrdUrd into newly synthesized DNA strands using the DELFIA cell proliferation kit (Perkin-Elmer) according to the manufacturer's instructions on a Wallac Victor^2 multilabel counter (Perkin-Elmer). All assays were done in triplicates and repeated twice.

Cell cycle analysis. Twenty-four hours after transfection with siRNA duplexes, 1×10^5 cells were cultured in serum-free medium for 12 h. Forty-eight hours after medium was supplemented with EGF (50 nmol/L), cells were harvested, ethanol fixed, and stained with propidiumiodide before flowcytometric DNA content analysis. Cells in the different phases of the cell cycle were quantified using FlowJo (Tree Star) flowcytometric analysis software. All assays were done in triplicates and repeated twice.

Cell migration and *in vitro* invasion assay. Cell motility (chemokinesis) assays were conducted in transwell chambers with 8.0-μm pore membranes (BD Biosciences) with cells cultured in medium with various concentrations of EGF. Twenty-four hours after transfection with siRNA duplexes, cells were cultured in serum-free medium for 12 h and 4×10^4 cells were added to the top chamber. The top and bottom chamber both contained medium with equal concentrations of EGF (50, 10, 2, or 0.4 nmol/L). Twenty-four hours later, cells that had migrated to the bottom side of the membrane were fixed in ice-cold methanol. Membranes were excised, placed on microscope slides, and mounted with Hoechst (Dako) for fluorescence microscopy. Cells in five random visual fields (magnification, ×100) were counted for each membrane. All experiments were done in triplicates. For *in vitro* invasion assays, the top chambers were prepared with 100 μL of Matrigel (BD Biosciences) diluted to 1 mg/mL in serum-free medium. Chambers were incubated for 5 h at 37°C for gelling. All assays were done in triplicates and repeated twice.

Statistics. Correlation analysis of normalized MS4A12 mRNA expression levels in colon cancer samples with tumor stage and grading was done using Kruskal-Wallis nonparametric ANOVA test with GraphPad Prism software package (GraphPad Software). The statistical significance of MS4A12 silencing on proliferation, cell cycle progression, migration, and invasion of LoVo cells was calculated using unpaired t test with GraphPad Prism software package (GraphPad Software), comparing effects in siRNA treated cells with untreated cells.

Results and Discussion

We applied a genome-wide data mining strategy to search for targets for mAb therapy of colon cancer. Our approach was based on digital cDNA library subtraction to discover differentiation genes with exquisite specificity for colonic epithelial cells

[4] ftp://ncbi.nlm.nih.gov/repository/dbEST
[5] http://www.ncbi.nlm.nih.gov/BLAST
[6] http://smart.embl-heidelberg.de

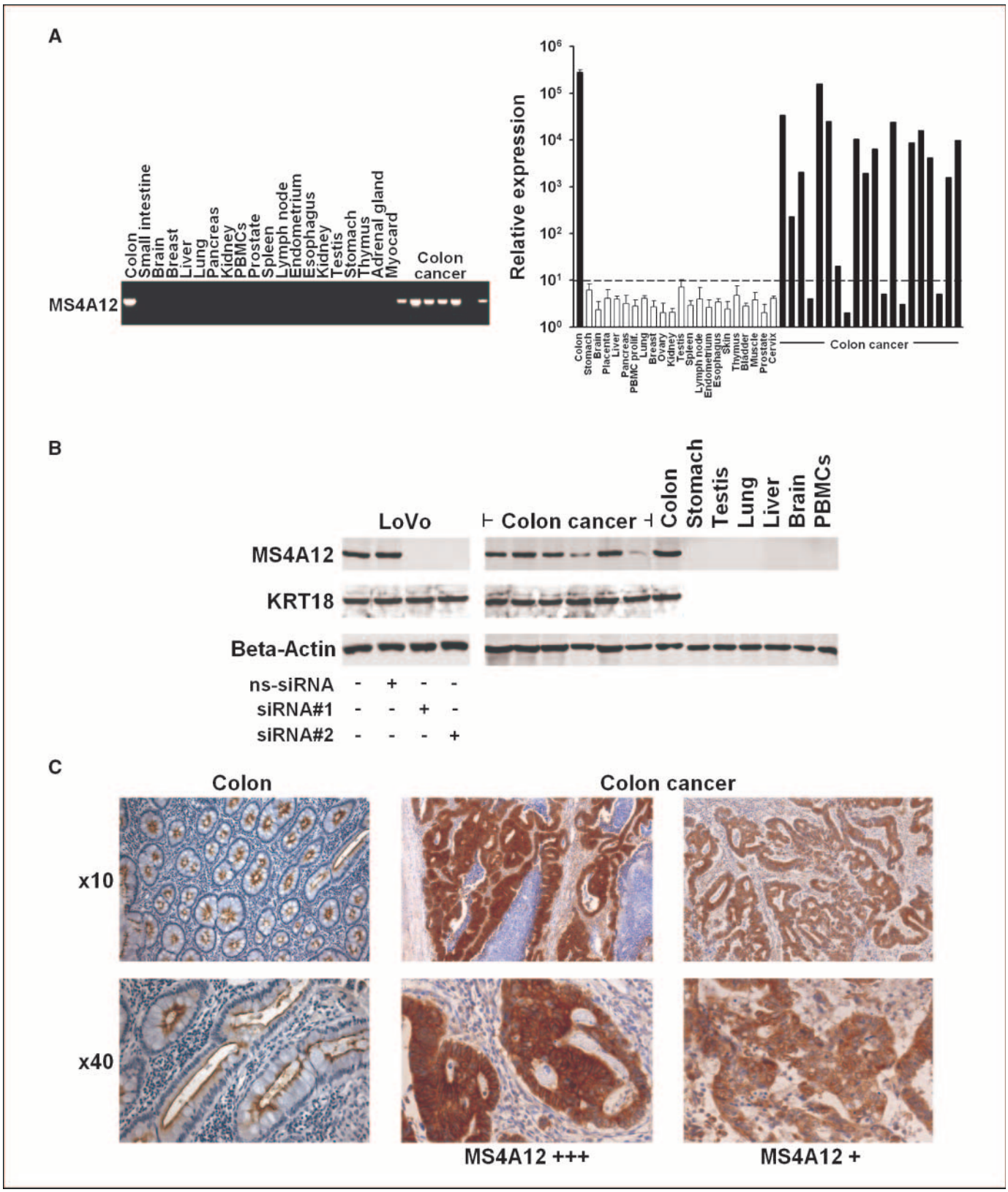

Figure 1. MS4A12 expression is restricted to normal colonic mucosa and colon cancer. *A,* end point RT-PCR (*left*) and quantitative real-time RT-PCR (*right*) of *MS4A12* in normal tissues and colon cancer. For each normal tissue, the mean expression values of up to five individual tissue specimens are shown. *Columns,* mean; *bars,* SD; *dashed line,* expression cutoff. *B,* silencing of MS4A12 protein expression in LoVo colon cancer cells 48 h after transfection with two individual siRNA duplexes. *ns-siRNA,* nonsilencing siRNA (*left*). MS4A12 protein expression in normal tissues and colon cancer was detected with anti–MS4A12/N-term antiserum (*right*). β-Actin was used as loading control and Cytokeratin18 (KRT18) was used as a marker specific for epithelial cells. *C,* immunohistochemical detection of MS4A12 protein expression in normal colon and colon cancers with high (MS4A12+++) and low (MS4A12+) expression.

structurally resembling the CD20 protein with at least four hydrophobic regions qualifying as transmembrane domains. Such candidates were subsequently tested for conserved expression in cancers derived from this lineage. One of the hits of our computational screen perfectly complying with our search criteria was MS4A12. This molecule is in fact a member of the MS4A family comprising structurally related cell surface proteins such as CD20 (MS4A1), the high-affinity IgE receptor β chain (FcεRIβ; MS4A2), and HTm4 (MS4A3; refs. 20–22). In contrast to the majority of members of the *MS4A* family, which have been previously shown to be differentiation genes of hematopoetic or lymphatic cell lineages, *MS4A12* has not been detected in such cells (21, 22).

To determine, which human tissues express *MS4A12*, we profiled a comprehensive set of 27 different normal human tissue specimens from up to five donors per tissue type by specific end point and quantitative real-time RT-PCR. Tissues were classified as negative in case of lack of a visible amplification product in end point RT-PCR and if not exceeding the cutoff of mean expression in all normal noncolonic tissue samples + 3STDs (99% percentile). We found *MS4A12* expression to be confined to normal colon mucosa. In all other normal tissues, transcript levels were below the detection limit of standard 35 cycle RT-PCR (Fig. 1*A, left*) and only trace amounts of *MS4A12* transcripts could be detected after 40 cycles of quantitative real-time RT-PCR (Fig. 1*A, right*) with only 1 of 5 testis specimens slightly exceeding the expression cutoff (Table 1).

Profiling of tumor specimens revealed that 25 of 40 (63%) colon cancers expressed *MS4A12*. In order not to overestimate expression frequency of *MS4A12* as measured by qPCR in colon cancer samples, we classified transcript levels of at least 10-fold above normal tissue cutoff as positive (Supplementary Table S1). Within the sample population, expression levels of *MS4A12* did not correlate with tumor stage or tumor grade ($P = 0.68$ and $P = 0.36$; Kruskal-Wallis). *MS4A12* was not detected in any other human tumor type including breast cancer, lung cancer, prostate cancer, gastric cancer, renal cell cancer, malignant melanoma, hepatocellular cancer, leukemia, and head neck cancer (Table 1).

For analysis of protein expression, we used an affinity purified polyclonal rabbit antibody (anti–MS4A12/N-term) raised against a recombinantly expressed polypeptide corresponding to the NH_2 terminal 63 amino acids of MS4A12. To verify specificity of the antibody, we used gene silencing of MS4A12 by siRNA. Transfection of MS4A12-expressing colon cancer cell line LoVo with two individual MS4A12-specific siRNA duplexes resulted in stable and reproducible reduction of constitutive *MS4A12* mRNA expression by 90%, whereas scrambled nonsilencing control duplexes had no effect (Supplementary Fig. S1). Consistent with this observation, the ~35-kDa band, detected in accordance with the predicted size of MS4A12 in lysates of LOVO cells in Western blot, disappeared completely (Fig. 1*B*). This proved both robust knockdown of MS4A12 protein expression as well as specificity of the antibody. Western Blot staining of MS4A12 protein in primary human tissue samples with anti–MS4A12/N-term confirmed MS4A12 protein expression in colon cancer specimens in levels comparable with normal colon mucosa as the only expressing normal tissue but not in tissues typed negative by RT-PCR. Normalization to cytokeratin-18 (KRT18) as a marker for epithelial cells ruled out that high MS4A12 protein levels in colon cancers were observed as a result of a higher portion of epithelial cells in the specimen.

Table 1. Expression of MS4A12 in tissues typed by quantitative real-time RT-PCR

Normal tissues	Positive/tested
Colon	5/5
Stomach	0/5
Brain	0/3
Placenta	0/5
Liver	0/5
Pancreas	0/5
PBMCs, resting	0/5
PBMCs, proliferating	0/5
Lung	0/5
Breast	0/5
Ovary	0/5
Kidney	0/5
Testis	1/5
Spleen	0/5
Lymph node	0/5
Endometrium	0/5
Esophagus	0/5
Skin	0/3
Thymus	0/2
Bladder	0/3
Muscle	0/3
Prostate	0/5
Cervix	0/5
Adrenal gland	0/3
Small intestine	0/4
Tonsil	0/5
Myocard	0/2
Cancerous tissues	
Colon cancer	25/40
Breast cancer	0/20
Lung cancer	0/20
Prostate cancer	0/15
Gastric cancer	0/15
Renal cell cancer	0/15
Malignant melanoma	0/10
Hepatocellular cancer	0/10
Leukemia	0/10
Head/neck cancer	0/5

NOTE: Specimens obtained from two to five different individuals were investigated per normal tissue type. Cutoff for normal tissues was set to mean expression in normal tissues, except colon, +3 SD (relative expression of 10-fold above detection limit). In tumor tissues, only expression values at least 100-fold above detection limit were scored positive.
Abbreviation: PBMC, peripheral blood mononuclear cells.

Immunohistochemistry with anti–MS4A12/N-term antibody on normal colon mucosa revealed a characteristic and distinct apical membrane staining of the epithelial cells of normal colonic crypts (Fig. 1*C*). In sections obtained from other gastrointestinal tissues and testis MS4A12 staining was not detectable (Supplementary Fig. S2), excluding that smaller subpopulations present within these composite organ tissues do express this protein. In colon cancer, only the neoplastic cell population was stained, whereas adjacent

stromal and nonneoplastic epithelial cells were negative. Although additional cytoplasmic immunostaining was observed, staining of tumor cells was clearly accentuated at the plasma membrane, substantiating predictions that MS4A12 is a cell surface protein (22). In the pilot set of stained colon cancer samples, tumors with homogenous and strong expression, as well as specimens with weaker and more heterogeneous expression were observed (Fig. 1*C*).

Membrane topology of CD20 as prototypic member of the MS4A family has been extensively characterized. CD20 is a 297 amino acid protein with cytoplasmic aminoterminal and carboxyterminal ends and four transmembrane domains forming two extracellular loops (6). As there is a considerable sequence identity among MS4A family members (Supplementary Fig. S3*A*), it has been predicted that other MS4A proteins share the surface localization and peculiar topology of CD20 (22). Alignment of the MS4A12 protein sequence with the CD20 domain (pfam04103) showed a 43% sequence similarity on the amino acid level (Supplementary Fig. S3*B*). Analogous to reports for other MS4A12 family members, the highest degree of identity was found in the first three transmembrane stretches (22), and a tetraspan membrane topology was predicted (Fig. 2*A*). Cell membrane localization was experimentally confirmed by immunofluorescence microscopy of Chinese hamster ovary (CHO) cells transfected with eGFP-tagged MS4A12 constructs (Fig. 2*B*). Further support was provided by the distinct plasma membrane staining of LoVo colon cancer cells constitutively expressing MS4A12 by anti–MS4A12/N-term antibody, which was lost upon siRNA-induced knockdown of MS4A12 (Fig. 2*C*). To verify the predicted topology, CHO cells were transfected with MS4A12 constructs tagged either NH_2 or COOH terminally with eGFP and stained with anti-eGFP antibodies after paraformaldehyde fixation. Both NH_2 and COOH terminally localized eGFP was only detectable by flowcytometric analysis after permeabilization of transfected cells with saponin (Fig. 2*D*) but not under conditions impairing penetration of the antibody into the cells. In summary, these data support cell surface localization of MS4A12 as well as the predicted topology with intracellular localization of the NH_2 and COOH terminus.

As CD20 has been shown to possess SOC channel (SOCC) activity (23), we hypothesized that MS4A12 may also be involved in capacitative calcium entry. CHO cells transfected either with an MS4A12-encoding plasmid or with the empty vector as control were treated with thapsigargin, a specific inhibitor of the endoplasmic reticular Ca^{2+}-ATPase to deplete intracellular calcium stores (24). In addition to Ca^{2+} entry, we also tested Sr^{2+} influx, as Sr^{2+} entry can potentially distinguish between endogenous and exogenously expressed SOC channels (23, 25). Baseline Ca^{2+} levels as measured by fluorescence detection of a Ca^{2+}-sensitive dye were identical in control and in MS4A12-expressing CHO cells (Fig. 3*A*). As expected, thapsigargin sharply increased $[Ca^{2+}]_c$ in the absence of extracellular Ca^{2+} in both cell lines. $[Ca^{2+}]_c$ gradually returned to baseline levels, most likely due to extrusion mechanisms at the plasma membrane and by uptake into internal organelles (26). Subsequent perfusion of cells with Sr^{2+} induced a considerable fluorescence increase in MS4A12-transfected cells, suggesting that influx of Sr^{2+} occurred in response to store depletion. Vector-transfected cells did not respond to Sr^{2+}, indicating that endogenous SOC channels are impermeable to Sr^{2+} under the experimental conditions. No Sr^{2+} entry occurred before store depletion, indicating that MS4A12 expression does not confer constitutive permeability to Sr^{2+} in CHO cells. After Sr^{2+} was withdrawn and fluorescence values had returned to baseline, Ca^{2+} was introduced into the perfusion chamber. Influx of Ca^{2+} into vector-transfected cells indicated that these cells maintained a

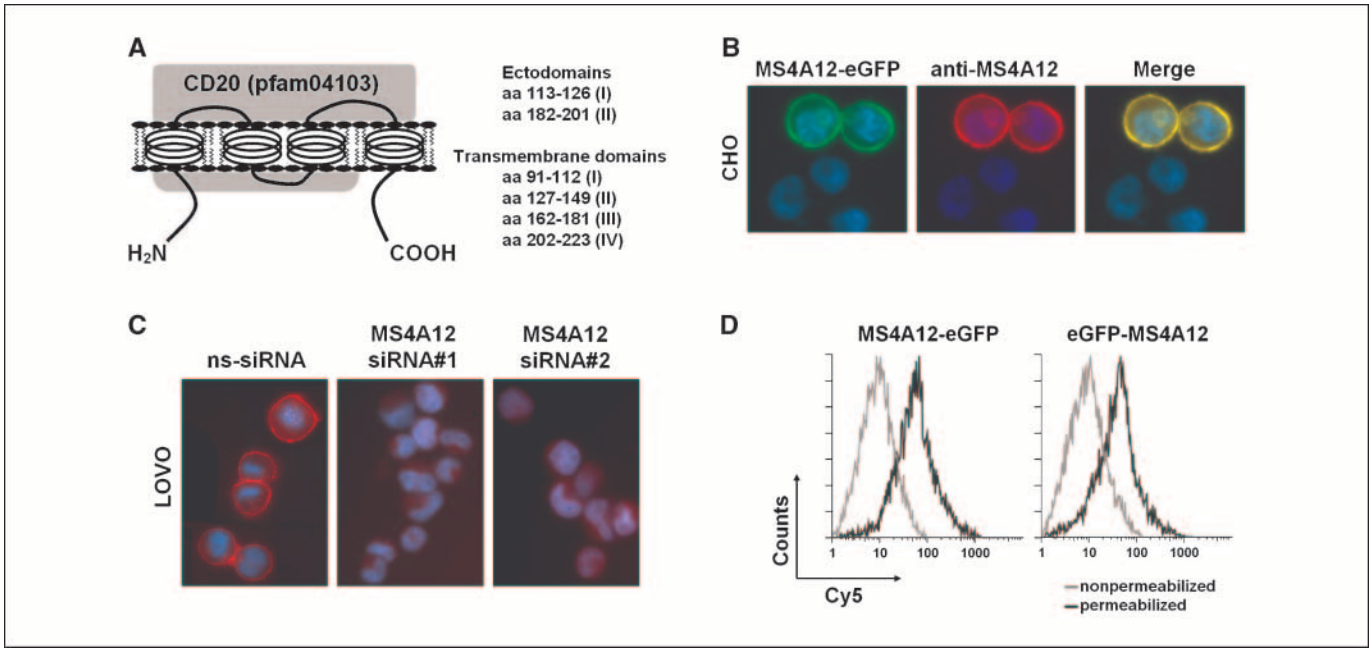

Figure 2. MS4A12 is a CD20-like plasma membrane protein. *A,* predicted plasma membrane topology of MS4A12. The region with high homology to CD20 is boxed gray. *B,* IF microscopic analysis of CHO cells transfected with MS4A12-eGFP stained with anti–MS4A12/N-term antiserum. *C,* immunofluorescence microscopic analysis of LoVo cells stained with anti–MS4A12/N-term 48 h after transfection with control siRNA or MS4A12-specific siRNAs. *D,* flowcytometric analysis of CHO cells transfected with NH_2 or COOH terminally eGFP-tagged MS4A12. Nonpermeabilized and permeabilized cells were stained with a rabbit polyclonal anti-eGFP antibody and an anti-rabbit Cy5-labeled secondary antibody.

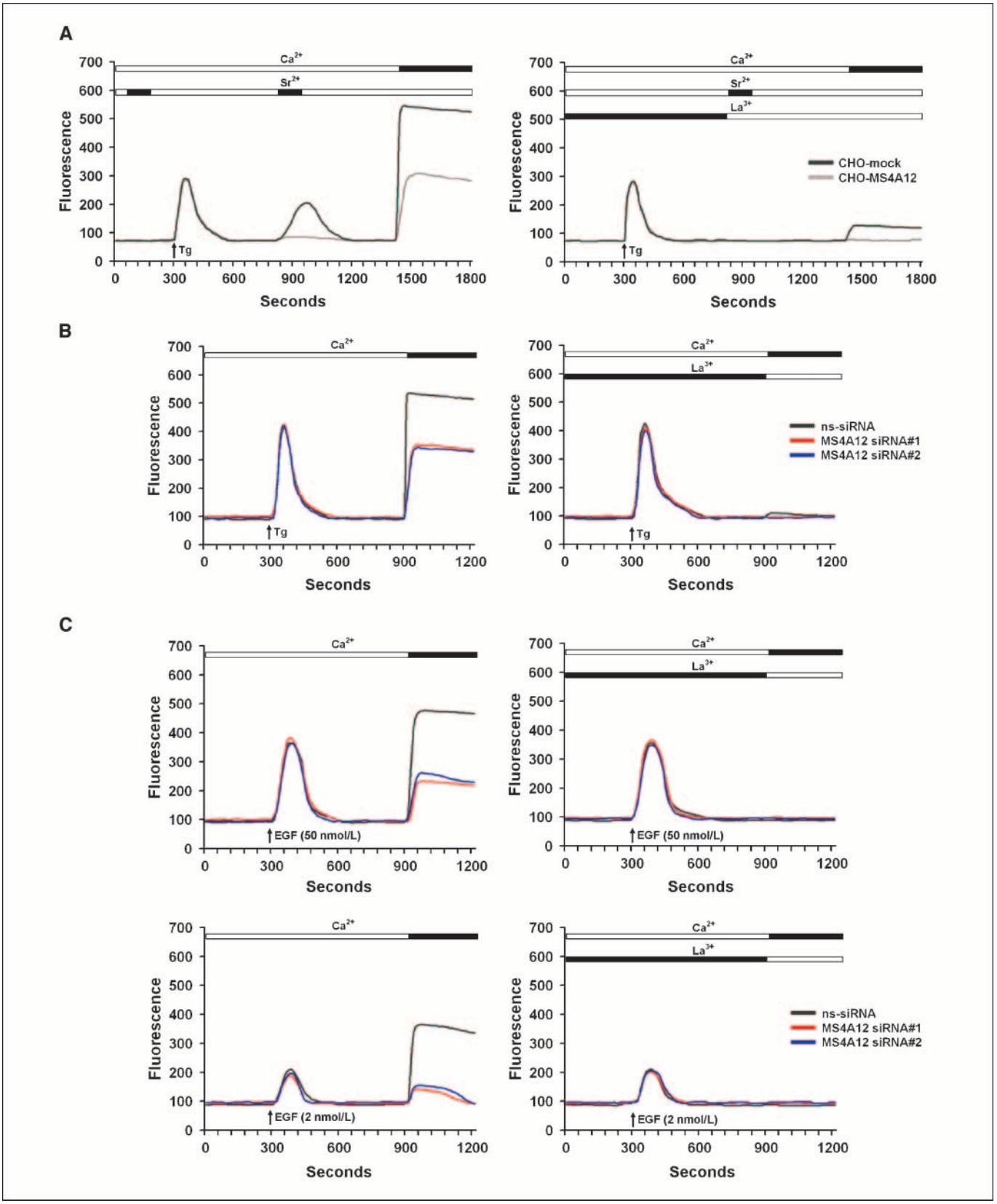

Figure 3. Store-operated calcium entry mediated by MS4A12. *A,* Ca^{2+} (1 mmol/L) and Sr^{2+} (1 mmol/L) entry in CHO cells transfected with MS4A12 or with vector alone as control was measured after Ca^{2+} store depletion with thapsigargin (300 nmol/L) without (*left*) and with (*right*) pretreatment of cells with known SOC blocker La^{3+} (25 μmol/L). *B,* Ca^{2+} (1 mmol/L) entry in LoVo cells after Ca^{2+} store depletion with thapsigargin (300 nmol/L) without (*left*) and with (*right*) pretreatment of cells with La^{3+} (25 μmol/L). *C,* Ca^{2+} entry measured after Ca^{2+} store depletion in response to EGF (50 nmol/L, *top row*; 2 nmol/L, *bottom row*) without (*left*) and with (*right*) pretreatment of cells with La^{3+} (25 μmol/L). Shown are representative results of three independent experiments done in triplicate.

normal Ca^{2+} entry pathway after thapsigargin treatment. Calcium influx into MS4A12-transfected cells was significantly increased over that observed in vector-transfected cells. Pretreatment of cells with the known SOC channel blocker La^{3+} resulted in marked reduction of Ca^{2+} influx into MS4A12-transfected cells, which in control cells was not detectable at all (Fig. 3*A*). Sr^{2+} entry in both cell lines was completely abolished. In summary, these data suggest that MS4A12 has the ability to form and/or organize a SOC entry pathway.

Ca^{2+} flux is the fastest response after activation of receptor tyrosine kinases (27, 28). Binding of growth factors, such as EGF, to their receptors on the plasma membrane leads to activation of phospholipase C γ (PLCγ) that hydrolyzes membrane lipids to produce inositol 1,4,5-trisphophate (IP_3). IP_3 binds to the IP_3 receptor located on the membrane of the endoplasmic reticulum (ER) and stimulates Ca^{2+} release into the cytoplasm. This, in turn, is associated with SOC entry. For functions, for which prolongation of the Ca^{2+} signal plays an important role such as cell growth, SOC entry is a major component of calcium signaling (15, 16). To assess the role of MS4A12 in calcium entry in response to growth factor signaling, we used MS4A12-positive LoVo colon cancer cells, which express high levels of EGFR (29). Treatment of LoVo cells with EGF has been shown to induce SOC entry in a PLCγ-dependent manner (27, 30–32). LoVo cells transfected with MS4A12-specific siRNAs or scrambled control siRNA were treated with thapsigargin and two different concentrations of EGF. Again, no difference in baseline fluorescence was detected. In both cell lines, thapsigargin as well as EGF both sharply increased $[Ca^{2+}]_c$ in the absence of extracellular Ca^{2+}. SOC entry, however, was significantly impaired in cells with MS4A12 expression knockdown but not in cells transfected with control siRNA (Fig. 3*B* and *C*). Pretreatment of both cell lines with La^{3+} inhibited SOC entry completely. Noteworthy, Ca^{2+} entry in cells treated with low concentrations of EGF (2 nmol/L) was nearly completely abolished by MS4A12 silencing. According to these data, SOC entry in LoVo cells is at least partially mediated by MS4A12. The Ca^{2+} entry remaining after MS4A12 silencing indicates the presence of other SOCCs in this cell system.

Growth factor–induced signaling is often organized in an oscillatory pattern (27). Repetitive calcium spikes require both the entry of external calcium via SOCCs and its release from internal stores. This results in activation of immediate-early genes responsible for inducing resting cells (G_0) to reenter the cell cycle (33). Most interestingly, in clinical trials targeting SOC entry by Ca^{2+} influx inhibitors, tumor growth inhibition of certain cancers is observed (34, 35). Therefore, we assessed the effect of MS4A12 expression on the proliferation of LoVo cells in response to EGF. We observed a significant reduction of growth factor–induced cell proliferation in cells with siRNA-mediated silencing of MS4A12 compared with control cells (Fig. 4*A*). Cell cycle analysis revealed a distinct G_1-S arrest in cells transfected with MS4A12 siRNAs as the underlying cause for the proliferation block (Fig. 4*B*), whereas vitality of the cells was not affected (data not shown).

Another important cellular function tightly regulated by the availability of free cytoplasmic Ca^{2+} is growth factor–induced cell motility and migration (16). The increase in free cytoplasmic Ca^{2+} by InsP3-mediated release of Ca^{2+} from intracellular pools results in activation of the actin cytoskeleton in the immediate submembrane region (36), which is elementary for cell migration. We investigated the effect of MS4A12 on growth factor–mediated motility of LoVo cells in transwell migration assays. Baseline motility (chemokinesis) was assessed by adding various concentrations of EGF to both the top and bottom chamber of the system. Motility was significantly reduced upon knockdown of MS4A12 (Supplementary Fig. S3*A*; Fig. 5*A*). Chemoinvasive activity of cells, as well, as measured by their ability to break through a barrier of Matrigel to migrate along EGF gradients was profoundly affected and substantially impaired by MS4A12 knockdown (Supplementary Fig. S3*B*; Fig. 5*B*). Intriguingly, the effect of MS4A12 silencing on both cellular functions was particularly pronounced in cells exposed to low concentrations of EGF. Enhanced Ca^{2+} flux mediated by expression of MS4A12 seems to lower the threshold concentration of EGF required for the activation of the EGFR pathway.

In summary, we present here the first functional characterization of MS4A12. We reveal that MS4A12 is a component of SOC entry and modulates EGFR signaling in colon cancer cells. The strict restriction of expression to colonocytes implies a specialized role of MS4A12 in this tissue type. This is further supported by its involvement in modulation of EGFR signaling, which has a pivotal role in the development and maintenance of intestinal epithelial continuity and is involved in control of a variety of epithelial cell

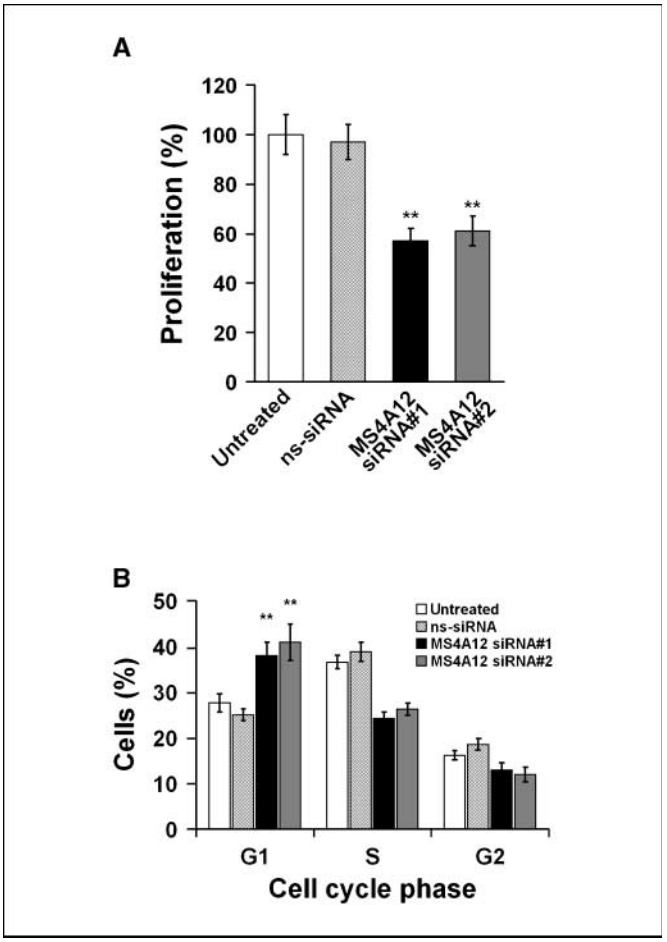

Figure 4. MS4A12 silencing impairs proliferation of LoVo colon cancer cells. *A,* 48 h after transfection with siRNAs, LoVo cells were cultured with 50 nmol/L EGF for 48 h. Proliferation was measured by incorporation of BrdUrd into newly synthesized DNA. *B,* cell cycle analysis of LoVo cells cultured under the same conditions shown as bar chart of cell fractions in different cell cycle states. All experiments were done in triplicate and repeated twice; *columns,* mean values of all experiments; *bars,* SD; *, $P < 0.05$; **, $P < 0.005$.

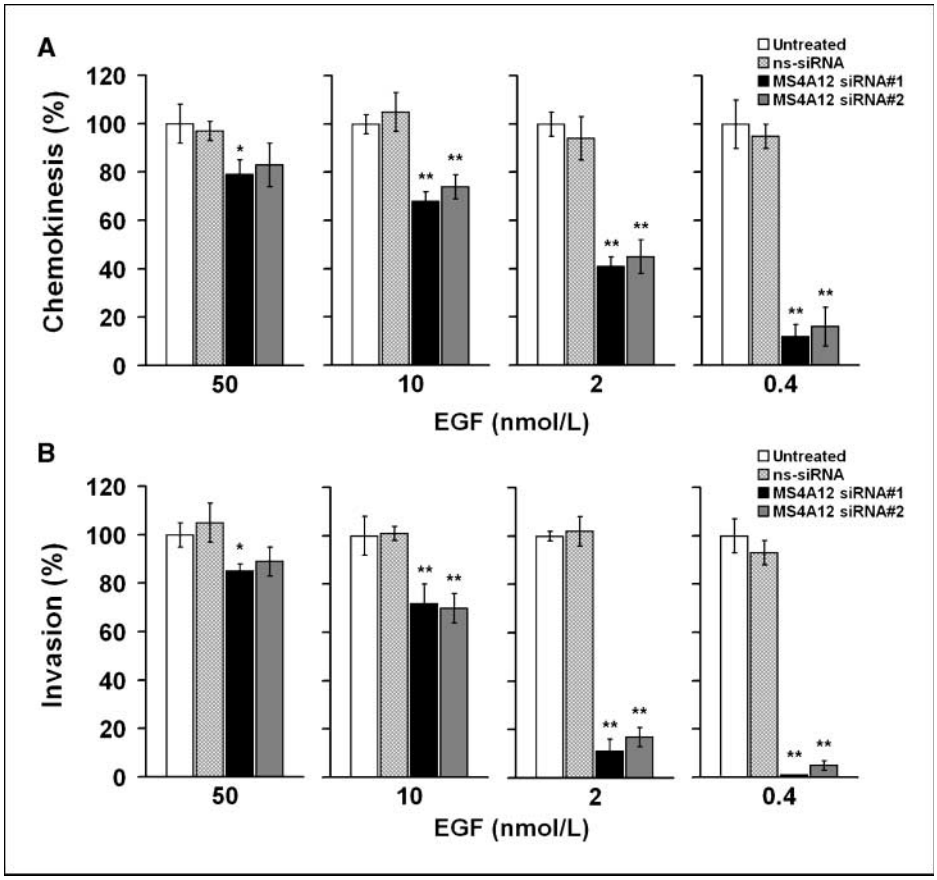

Figure 5. MS4A12 silencing impairs motility and invasion of LoVo colon cancer cells. *A,* chemokinesis (cell motility) was analyzed in transwell migration assays with various concentrations of EGF added to the top as well as the bottom chamber after 12 h. *B,* analysis of chemotactic invasion into Matrigel 24 h after various concentrations of EGF as chemoattractant have been added to the bottom chamber. Data are normalized to the nontransfected control cells for each concentration of EGF to emphasize that MS4A12 knockdown has the most prominent effect on motility and invasion at low EGF concentrations. All experiments were done in triplicate and repeated twice; *columns,* mean; *bars,* SD; *, $P < 0.05$; **, $P < 0.005$.

properties, such as growth, healing, adhesion, and cell migration (37–40). Other growth factors and peptides involved in these functions (e.g., transforming growth factor α and intestinal trefoil factor) all act, at least partially, via the EGFR signaling pathway (41). Whereas most cognate receptors are on the epithelial basolateral surface, cytoprotective trefoil peptides are secreted onto the apical surface of the mucosa (42, 43). It is tempting to speculate that the spatially restricted expression of MS4A12 in the apical epithelial monolayer might render these cells more sensitive to the cytoprotective action of such factors. MS4A12 expression is maintained upon malignant transformation and is detectable in a significant portion of colon cancers. As modulator of EGFR signaling, which is the dominant tumor-promoting factor in colon cancer, it is linked to features contributing to the tumor phenotype such as survival, proliferation, and motility as partially supported by our siRNA data. The observation that loss of MS4A12 impairs such EGFR-dependent cell functions, whereas expression of MS4A12 lowers the threshold for EGF-triggered Ca^{2+} entry may have clinical effects. Ongoing studies have to assess whether MS4A12 expression status of colon cancer patients affects sensitivity of their cancer cells to EGF and thereby prognosis of the patients. Moreover, correlation of response of patients to treatment with antibodies against EGFR, such as Erbitux, with MS4A12 status of their tumors will be part of ongoing work.

Several findings qualify MS4A12 as a novel target candidate for therapeutic antibodies.

First, being a lineage-specific marker highly selective for colonic epithelia, MS4A12 is absent from other toxicity-relevant normal tissues. Despite their expression in normal colonic mucosa, mAbs targeting differentiation antigens in colon cancer can be safely administered without inducing toxic side effects in the normal mucosa (44), most likely resulting from the high colonocyte turnover (45), counteracting accumulation of the antibody in normal mucosa. The narrow spatial expression pattern of MS4A12 in the most apical region of the normal mucosa should further add to the safety of MS4A12-targeting antibodies.

Second, MS4A12 expression is maintained in a significant portion of colon cancers. Large-scale analysis of colon cancer specimens by immunohistochemistry are under way to assess the prevalence of MS4A12 protein expression and homogeneity of this target candidate in individual tumor specimens, which will assist in judging the suitability of the molecule for targeted therapy.

Third, MS4A12 is a surface molecule and is therefore potentially drugable by antibodies. Sequence similarity to other MS4A family members and our experimental data suggest that MS4A12, such as CD20, might be embedded into the plasma membrane with two extracellular loops. The consequence of this particular topology would be that (*a*) shedding of the antigen is prevented, (*b*) binding mAbs are highly concentrated in small areas of the plasma membrane, and that (*c*) there is a short distance between the target epitope and the cell surface. These features have been reported to enhance the ability of mAbs to induce efficient recruitment of cytotoxic immune effector mechanisms (46–48). The structural similarity to CD20 makes it likely that antibodies exhibiting recruitment of complement and FcR-positive effector cells can be engineered. Its link to EGFR signaling positions MS4A12 in a pathway that is already being addressed by a variety of mAbs and small compounds. Many of these therapies are approved or are

currently in advanced clinical development, which adds to its attractiveness as drug target.

The data we present here suggest that MS4A12 might bear a therapeutic potential as antibody target in colon cancer. Ongoing work in our laboratory assesses whether mAbs generated against this target have the expected functional characteristics and may be of therapeutic value.

Acknowledgments

Received 10/5/2007; revised 1/17/2008; accepted 2/21/2008.

Grant support: Combined Project Grant SFB 432, the Heisenberg scholarship TU 115/2-1 of the Deutsche Forschungsgemeinschaft, and the MAIFOR program of the Johannes Gutenberg-University.

The costs of publication of this article were defrayed in part by the payment of page charges. This article must therefore be hereby marked *advertisement* in accordance with 18 U.S.C. Section 1734 solely to indicate this fact.

References

1. Glennie MJ, van de Winkel JG. Renaissance of cancer therapeutic antibodies. Drug Discov Today 2003;8:503–10.
2. Countouriotis A, Moore TB, Sakamoto KM. Cell surface antigen and molecular targeting in the treatment of hematologic malignancies. Stem Cells 2002;20:215–29.
3. Dillman RO. Monoclonal antibody therapy for lymphoma: an update. Cancer Pract 2001;9:71–80.
4. Leget GA, Czuczman MS. Use of rituximab, the new FDA-approved antibody. Curr Opin Oncol 1998;10:548–51.
5. Leonard JP. Targeting CD20 in Follicular NHL: novel anti-CD20 therapies, antibody engineering, and the use of radioimmunoconjugates. Hematology (Am Soc Hematol Educ Program) 2005;335–9.
6. Cartron G, Watier H, Golay J, Solal-Celigny P. From the bench to the bedside: ways to improve rituximab efficacy. Blood 2004;104:2635–42.
7. Cragg MS, Morgan SM, Chan HT, et al. Complement-mediated lysis by anti-CD20 mAb correlates with segregation into lipid rafts. Blood 2003;101:1045–52.
8. Cragg MS, Glennie MJ. Antibody specificity controls *in vivo* effector mechanisms of anti-CD20 reagents. Blood 2004;103:2738–43.
9. Johnson P, Glennie M. The mechanisms of action of rituximab in the elimination of tumor cells. Semin Oncol 2003;30:3–8.
10. Deans JP, Li H, Polyak MJ. CD20-mediated apoptosis: signalling through lipid rafts. Immunology 2002;107:176–82.
11. Shan D, Ledbetter JA, Press OW. Apoptosis of malignant human B cells by ligation of CD20 with monoclonal antibodies. Blood 1998;91:1644–52.
12. Shan D, Ledbetter JA, Press OW. Signaling events involved in anti-CD20-induced apoptosis of malignant human B cells. Cancer Immunol Immunother 2000;48:673–83.
13. Unruh TL, Li H, Mutch CM, et al. Cholesterol depletion inhibits src family kinase-dependent calcium mobilization and apoptosis induced by rituximab crosslinking. Immunology 2005;116:223–32.
14. Berridge MJ. Elementary and global aspects of calcium signalling. J Physiol 1997;499:291–306.
15. Berridge MJ, Bootman MD, Lipp P. Calcium-a life and death signal. Nature 1998;395:645–8.
16. Berridge MJ, Lipp P, Bootman MD. The versatility and universality of calcium signalling. Nat Rev Mol Cell Biol 2000;1:11–21.
17. Ghetie MA, Bright H, Vitetta ES. Homodimers but not monomers of Rituxan (chimeric anti-CD20) induce apoptosis in human B-lymphoma cells and synergize with a chemotherapeutic agent and an immunotoxin. Blood 2001;97:1392–8.
18. Hofmeister JK, Cooney D, Coggeshall KM. Clustered CD20 induced apoptosis: src-family kinase, the proximal regulator of tyrosine phosphorylation, calcium influx, and caspase 3-dependent apoptosis. Blood Cells Mol Dis 2000;26:133–43.
19. Koslowski M, Bell C, Seitz G, et al. Frequent nonrandom activation of germ-line genes in human cancer. Cancer Res 2004;64:5988–93.
20. Ishibashi K, Suzuki M, Sasaki S, Imai M. Identification of a new multigene four-transmembrane family (MS4A) related to CD20, HTm4 and β subunit of the high-affinity IgE receptor. Gene 2001;264:87–93.
21. Liang Y, Buckley TR, Tu L, Langdon SD, Tedder TF. Structural organization of the human MS4A gene cluster on Chromosome 11q12. Immunogenetics 2001;53:357–68.
22. Liang Y, Tedder TF. Identification of a CD20-, FcεRIβ-, and HTm4-related gene family: sixteen new MS4A family members expressed in human and mouse. Genomics 2001;72:119–27.
23. Li H, Ayer LM, Lytton J, Deans JP. Store-operated cation entry mediated by CD20 in membrane rafts. J Biol Chem 2003;278:42427–34.
24. Thastrup O, Cullen PJ, Drobak BK, Hanley MR, Dawson AP. Thapsigargin, a tumor promoter, discharges intracellular Ca2+ stores by specific inhibition of the endoplasmic reticulum Ca2(+)-ATPase. Proc Natl Acad Sci U S A 1990;87:2466–70.
25. Ma HT, Patterson RL, van Rossum DB, Birnbaumer L, Mikoshiba K, Gill DL. Requirement of the inositol trisphosphate receptor for activation of store-operated Ca2+ channels. Science 2000;287:1647–51.
26. Bootman MD, Collins TJ, Peppiatt CM, et al. Calcium signalling-an overview. Semin Cell Dev Biol 2001;12:3–10.
27. Munaron L. Calcium signalling and control of cell proliferation by tyrosine kinase receptors (review). Int J Mol Med 2002;10:671–6.
28. Patterson RL, van Rossum DB, Nikolaidis N, Gill DL, Snyder SH. Phospholipase C-γ: diverse roles in receptor-mediated calcium signaling. Trends Biochem Sci 2005;30:688–97.
29. Pai R, Soreghan B, Szabo IL, Pavelka M, Baatar D, Tarnawski AS. Prostaglandin E2 transactivates EGF receptor: a novel mechanism for promoting colon cancer growth and gastrointestinal hypertrophy. Nat Med 2002;8:289–93.
30. Kokoska ER, Smith GS, Miller TA. Nonsteroidal anti-inflammatory drugs attenuate proliferation of colonic carcinoma cells by blocking epidermal growth factor-induced Ca++ mobilization. J Gastrointest Surg 2000;4:150–61.
31. Kokoska ER, Wolff AB, Smith GS, Miller TA. Epidermal growth factor-induced cytoprotection in human intestinal cells involves intracellular calcium signaling. J Surg Res 2000;88:97–103.
32. Ma R, Sansom SC. Epidermal growth factor activates store-operated calcium channels in human glomerular mesangial cells. J Am Soc Nephrol 2001;12:47–53.
33. Berridge MJ. Calcium signalling and cell proliferation. BioEssays 1995;17:491–500.
34. Kohn EC, Reed E, Sarosy G, et al. Clinical investigation of a cytostatic calcium influx inhibitor in patients with refractory cancers. Cancer Res 1996;56:569–73.
35. Wasilenko WJ, Palad AJ, Somers KD, et al. Effects of the calcium influx inhibitor carboxyamido-triazole on the proliferation and invasiveness of human prostate tumor cell lines. Int J Cancer 1996;68:259–64.
36. Feldner JC, Brandt BH. Cancer cell motility-on the road from c-erbB-2 receptor steered signaling to actin reorganization. Exp Cell Res 2002;272:93–108.
37. Carpenter G, Cohen S. Epidermal growth factor. Annu Rev Biochem 1979;48:193–216.
38. Jones MK, Tomikawa M, Mohajer B, Tarnawski AS. Gastrointestinal mucosal regeneration: role of growth factors. Front Biosci 1999;4:303–9.
39. Lacy ER. Epithelial restitution in the gastrointestinal tract. J Clin Gastroenterol 1988;10:72–7.
40. Tarnawski AS, Jones MK. The role of epidermal growth factor (EGF) and its receptor in mucosal protection, adaptation to injury, and ulcer healing: involvement of EGF-R signal transduction pathways. J Clin Gastroenterol 1998;27:12–20.
41. Giraud AS. X. Trefoil peptide and EGF receptor/ligand transgenic mice. Am J Physiol Gastrointest Liver Physiol 2000;278:501–6.
42. Chinery R, Cox HM. Modulation of epidermal growth factor effects on epithelial ion transport by intestinal trefoil factor. Br J Pharmacol 1995;115:77–80.
43. Podolsky DK. Healing the epithelium: solving the problem from two sides. J Gastroenterol 1997;32:122–6.
44. Scott AM, Lee FT, Jones R, et al. A phase I trial of humanized monoclonal antibody A33 in patients with colorectal carcinoma: biodistribution, pharmacokinetics, and quantitative tumor uptake. Clin Cancer Res 2005;11:4810–7.
45. Lipkin M, Sherlock P, Bell B. Cell proliferation kinetics in the gastrointestinal tract of man. II. Cell renewal in stomach, ileum, colon, and rectum. Gastroenterology 1963;45:721–9.
46. Bindon CI, Hale G, Waldmann H. Importance of antigen specificity for complement-mediated lysis by monoclonal antibodies. Eur J Immunol 1988;18:1507–14.
47. Borsos T, Rapp HJ. Complement fixation on cell surfaces by 19S and 7S antibodies. Science 1965;150:505–6.
48. Golan MD, Burger R, Loos M. Conformational changes in C1q after binding to immune complexes: detection of neoantigens with monoclonal antibodies. J Immunol 1982;129:445–7.

Correction: MS4A12 in Colon Cancer

In the article on MS4A12 in colon cancer in the May 1, 2008 issue of *Cancer Research* (1), there is an error in Fig. 3*A*. The corrected figure appears below.

1. Koslowski M, Sahin U, Dhaene K, Huber C, Türeci Ö. MS4A12 is a colon-selective store-operated calcium channel promoting malignant processes. Cancer Res 2008;68: 3458–66.

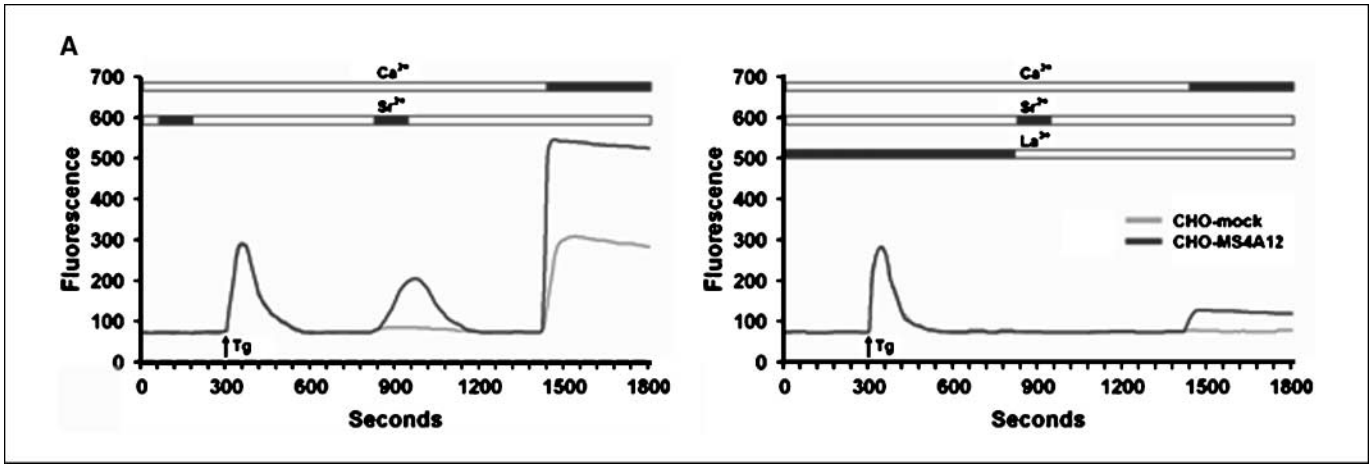

doi:10.1158/0008-5472.CAN-68-12-COR4

MS4A12 Is a Colon-Selective Store-Operated Calcium Channel Promoting Malignant Cell Processes

Michael Koslowski, Ugur Sahin, Karl Dhaene, et al.

Cancer Res 2008;68:3458-3466.